

Nuclear structure effects in the fusion of calcium isotopes

S. Landowne

Physik Department, Technische Universität München, D-8046 Garching, West Germany

C. H. Dasso and R. A. Broglia

The Niels Bohr Institute and Nordita, Blegdamsvej 17, DK-2100 Copenhagen Ø, Denmark

G. Pollarolo

*Istituto di Fisica Teorica dell'Università di Torino and
Istituto Nazionale di Fisica Nucleare, Sezione di Torino,
Torino, Italy*

(Received 22 October 1984)

Fusion reaction cross sections are calculated for the $^{40}\text{Ca} + ^{40,44,48}\text{Ca}$ systems taking into account their low lying collective excitations. The remaining differences with the low energy data are interpreted as being due to coupling effects of transfer reaction channels which increase strongly for the $^{40}\text{Ca} + ^{44,48}\text{Ca}$ cases. Estimates for the observable transfer cross sections are given.

Recently Beckerman and collaborators have reported on the fusion cross sections for $^{40}\text{Ca} + ^{40,44,48}\text{Ca}$ down to energies well below the Coulomb barrier.¹ This series is particularly interesting because of the variety of structure that occurs as the $f_{7/2}$ neutron shell is filled. In the present work we calculate these cross sections explicitly taking the low-lying excitations of the colliding nuclei into account.

We follow the method which was proposed in Ref. 2 and which we have previously used to study the Ni+Ni and Ar+Sn fusion reactions.³ Namely, we diagonalize the coupling matrix corresponding to the interacting system at the position of the barrier and calculate a weighted average of the transition probabilities for the resulting set of effective barriers. The reliability of this procedure was checked against full numerical coupled-channel calculations in Ref. 4. In addition, the results of several coupled-channel calculations carried out for the present case compared well to the simpler diagonalization scheme.

The coupling form factors were generated using the collective model and the deformation parameters deduced from the coupled-channel analysis of $^{16}\text{O} + ^{40,44,48}\text{Ca}$ inelastic scattering carried out in Ref. 5. The strongest transitions to

the ground state were used, as summarized in Table I. To specify the nuclear potential we used a Woods-Saxon parametrization and adjusted it to fit the fusion data above the barrier for $^{40}\text{Ca} + ^{40}\text{Ca}$ as shown in Fig. 1. The parameters are $V_0 = -53.2$ MeV, $r_0 = 1.192$ fm, $a_0 = 0.63$ fm. This results in the barrier height, radius, and curvature values of $V_b = 55.2$ MeV, $r_b = 9.70$ MeV, and $\epsilon = 0.61$ MeV, respectively. The empirical formulas for the barrier height and radius determined by Vaz, Alexander, and Satchler⁶ from systematics of fusion data give $V_b = 55.3$ MeV and $r_b = 9.66$ fm.

Normal parametrizations of the nuclear potential usually allow for an $A^{1/3}$ scaling in the radii parameters. However, a simple calculation shows that this would overpredict the higher energy data points for the $^{40}\text{Ca} + ^{44,48}\text{Ca}$ cases. To emphasize the constraint imposed by fitting the higher energy fusion data, we have simply kept the barrier parameters fixed for the calculations shown in Fig. 1. This is also in keeping with the fact that the mean square radii of the Ca isotopes display a behavior with mass number which is weaker than $A^{1/3}$ (cf. Ref. 7). Notice then that the no-coupling results (dashed curves) are the same in each case.

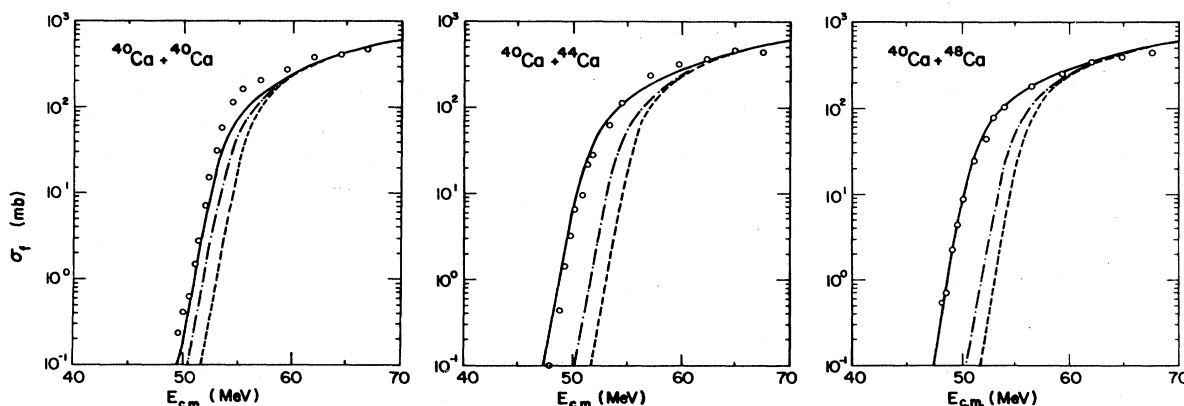


FIG. 1. Calculations for $^{40}\text{Ca} + ^{40,44,48}\text{Ca}$ fusion cross sections compared with the data of Ref. 1. The no-coupling limit (dashed curves) is fixed to be the same in each case. The dash-dotted curves include the couplings to the inelastic states in Table I. The solid curves include an additional "transfer" channel at $Q = -5$ MeV with strengths adjusted to fit the low energy data points.

TABLE I. Coupling scheme and deformation lengths (Ref. 5) used in the $^{40}\text{Ca} + ^{40,44,48}\text{Ca}$ fusion calculations.

Nucleus	Transition	ΔE (MeV)	δ_c (fm)	δ_N (fm)
^{40}Ca	$0^+ \rightarrow 3^-$	3.74	1.79	1.08
	$0^+ \rightarrow 5^-$	4.49	1.22	0.54
^{44}Ca	$0^+ \rightarrow 2^+$	1.16	1.08	0.85
	$0^+ \rightarrow 3^-$	3.31	0.87	0.60
	$0^+ \rightarrow 3^-$	4.40	0.48	0.45
^{48}Ca	$0^+ \rightarrow 2^+$	3.83	0.70	0.62
	$0^+ \rightarrow 3^-$	4.51	0.89	0.67

The dash-dotted curves in Fig. 1 show the results of including the inelastic couplings of Table I. It can be seen that a similar enhancement effect results in each case being slightly smaller for $^{40}\text{Ca} + ^{48}\text{Ca}$. It is clear from this comparison that the low energy $^{40}\text{Ca} + ^{44,48}\text{Ca}$ fusion cross sections are underpredicted much more severely than the $^{40}\text{Ca} + ^{40}\text{Ca}$ data. Thus, it does not seem possible to describe the measurements consistently through couplings to the strongest low-lying inelastic excitation channels.

This suggests that the discrepancies may be due to transfer reaction couplings which increase rapidly in the $^{40}\text{Ca} + ^{44,48}\text{Ca}$ cases. An increase in the transfer strength is also to be expected from considering the single particle levels near the Fermi surface. A count of the best-matched single neutron transfer possibilities with $Q \geq -7$ MeV gives 6 for $^{40}\text{Ca} + ^{40}\text{Ca}$ vs 14 for the $^{40}\text{Ca} + ^{44,48}\text{Ca}$ cases. Accordingly we introduced an additional channel at a typical Q value for neutron transfer ($Q \sim -5$ MeV) and adjusted the strength of the coupling to reproduce the low energy fusion cross sections, as shown by the solid curves in Fig. 1. The resulting strengths are $F_{40} = 2.0$ MeV, $F_{44} = 5.0$ MeV, and $F_{48} = 5.5$ MeV.

The transfer strength for $^{40}\text{Ca} + ^{40}\text{Ca}$ is comparable to the strength of the $0^+ \rightarrow 3^-$ transition in ^{40}Ca . We caution, however, that the absolute value for the transfer strength could be reduced by making adjustments in the inelastic coupling parameters. Notice, for instance, that the nuclear deformation lengths in Table I are smaller than the usual prescription of taking them equal to the Coulomb deformation lengths. We expect, however, that the relative transfer strengths for the different systems are more reliably given.

Predictions for the observable transfer cross sections for $^{40}\text{Ca} + ^{40,44}\text{Ca}$ are shown in Fig. 2. Here we have treated the additional "transfer" channel as a collective state and have used the coupled-channel code PTOLEMY⁸ with an ingoing boundary condition⁹ to calculate the reaction cross section in this channel. Notice that the cross sections scale approximately by the ratio of the squares of the coupling strengths. These results are in qualitative agreement with recent transfer reaction measurements.¹⁰

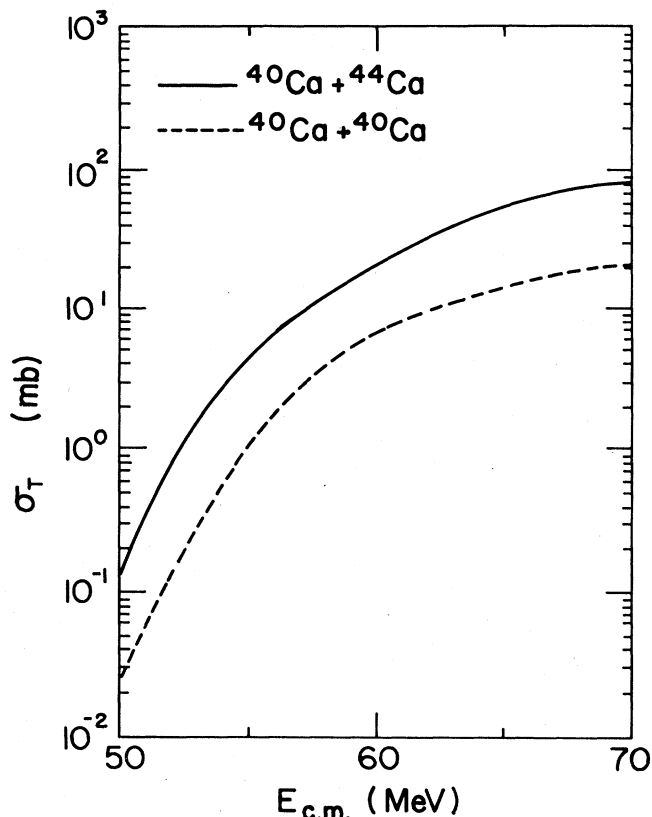


FIG. 2. Predictions for the total transfer reaction cross sections σ_T for $^{40}\text{Ca} + ^{40,44}\text{Ca}$ cases implied by the fits to the low energy fusion cross section data.

In summary, we have analyzed the $^{40}\text{Ca} + ^{40,44,48}\text{Ca}$ fusion reactions taking into account the effect of couplings to low-lying collective states. The above-barrier data seem to indicate that the nuclear potential is more stable than an $A^{1/3}$ radial scaling would imply. The subbarrier data for $^{40}\text{Ca} + ^{44,48}\text{Ca}$ are underpredicted when the calculations are constrained to fit the above-barrier data and only low-lying collective inelastic excitations are included. This is interpreted as being due to the coupling to a large number of transfer reaction channels in these cases. By fitting the low energy fusion data with an effective transfer coupling we have obtained predictions for the transfer reaction cross sections.

We thank M. Beckerman for communicating the fusion data to us prior to their publication. One of us (S.L.) has been supported by a grant of the Bundesministerium für Forschung und Technologie, Federal Republic of Germany.

¹H. Al-Juwait, R. Ledoux, M. Beckerman, E. Cosman, S. Gazes, M. Salomaa, J. Wiggins, R. Betts, S. Saini, and O. Hansen, *Bull. Am. Phys. Soc.* **28**, 670 (1983); *Phys. Rev. C* **30**, 1223 (1984).

²C. H. Dasso, S. Landowne, and A. Winther, *Nucl. Phys.* **A405**, 381 (1983); **A407**, 221 (1983).

³R. A. Broglia, C. H. Dasso, S. Landowne, and G. Pollaro, *Phys. Lett.* **133B**, 34 (1983).

⁴S. Landowne and S. C. Pieper, *Phys. Rev. C* **29**, 1352 (1984).

⁵K. E. Rehm, W. Henning, J. R. Erskine, D. G. Kovar, M. H.

Macfarlane, S. C. Pieper, and M. Rhoades-Brown, *Phys. Rev. C* **25**, 1915 (1983).

⁶L. C. Vaz, J. M. Alexander, and G. R. Satchler, *Phys. Rep.* **69**, 373 (1981).

⁷G. D. Alkazarov *et al.*, *Nucl. Phys.* **A280**, 365 (1977).

⁸M. Rhoades-Brown, M. H. Macfarlane, and S. C. Pieper, *Phys. Rev. C* **21**, 2417 (1980); **21**, 2436 (1980).

⁹S. C. Pieper (private communication).

¹⁰R. Ledoux and M. Beckerman (private communication).